ISA Transactions 138 (2023) 254–261

Contents lists available at ScienceDirect

ISA Transactions

journal homepage: www.elsevier.com/locate/isatrans

Research article

Abrupt moving target tracking based on quantum enhanced particle filter

Jiawang Wan [1], Cheng Xu [*,1], Weizhao Chen, Ran Wang, Xiaotong Zhang [*]

School of Computer and Communication Engineering, University of Science and Technology Beijing, Beijing, China
Shunde Innovation School, University of Science and Technology Beijing, Foshan, China

ARTICLE INFO

Article history:
Received 6 June 2022
Received in revised form 7 February 2023
Accepted 7 February 2023
Available online 10 February 2023

Keywords:
Target tracking
Quantum computation
Particle filter
Abrupt motion

ABSTRACT

Abrupt-motion tracking is challenging due to the target's unpredictable action. Although particle filter (PF) is suitable for target tracking of nonlinear non-Gaussian systems, it suffers from the problems of particle impoverishment and sample-size dependency. This paper proposed a quantum-inspired particle filter for abrupt-motion tracking. We apply the concept of quantum superposition to transform classical particles into quantum particles. Quantum representation and corresponding quantum operations are addressed to utilize quantum particles. The superposition property of quantum particles avoids the concerns of particle impoverishment and sample-size dependency. The proposed diversity-preserving quantum-enhanced particle filter (DQPF) obtains better accuracy and stability with fewer particles. A smaller sample size also helps to reduce computational complexity. Moreover, it has significant advantages for abrupt-motion tracking. The quantum particles are propagated at the prediction stage. They will exist at possible places when abrupt motion occurs, which reduces the tracking delay and enhances the tracking accuracy. This paper conducted experiments compared to state-of-the-art particle filter algorithms. The numerical results demonstrate that the DQPF is not susceptible to motion mode and particle number. Meanwhile, DQPF maintains excellent accuracy and stability.

1. Introduction

Target tracking is a crucial component in many essential services for the Internet-of-Things (IoT), such as surveillance, anomalous activity detection, and intelligent traffic management systems [1,2]. Especially abrupt-motion tracking is key and challenging due to its unpredictable nature, leading to the failure of most tracking methods. The Global Positioning System (GPS) attracts plentiful applications for outdoor navigation with its convenient and flexible characteristics [3]. However, it cannot provide accurate enough position estimation occasionally because of the relatively weak GPS signals impeded by dense structure materials. Classical Radio Frequency Identification (RFID) [4] based location method, such as time of arrival (ToA) [5], time difference of arrival (TDoA) [6] and received signal strength (RSS) [7], is an alternative in areas where GPS signals are unavailable. However, it is unsuitable for tracking in unknown areas due to its requirements for external infrastructure deployment.

Vision-based tracking methods, which extract features directly from the images to be augmented, usually obtain higher accuracy. However, according to Huber's theory of robust statistics, feature extraction's efficiency through the sequence severely limits their robustness [8], let alone the required external infrastructure deployment. On the other hand, vision-based methods are sensitive to partial occlusion, camera motion, and so on [9]. Researchers have come up with many methods to address this issue, including detection-based [10] and stochastic sampling-based tracking methods [11]. However, a pre-training procedure is required in detection-based tracking algorithms. Moreover, the stochastic sampling-based tracking algorithms track by stochastic sampling rather than a specific trajectory in the search space. These algorithms will introduce much time consumption.

On account of the relatively high accuracy and convenience, the inertial navigation system (INS) has been integrated into various devices [12]. However, as the critical component of INS, the inertial measurement unit (IMU) lacks long-term stability due to sensor noise, accumulative errors, and drifting [13]. The filtering method, especially the particle filter, which has superior adaptation to a nonlinear and non-Gaussian abrupt-motion tracker [14], provides a reliable solution for enhancing the performance of IMU. The process of particle filter is shown in Fig. 1, which is a continuous iterative process. However, a general particle filter

* Corresponding authors at: School of Computer and Communication Engineering, University of Science and Technology Beijing, Beijing 100083, China
E-mail addresses: xucheng@ustb.edu.cn (C. Xu), zxt@ies.ustb.edu.cn (X. Zhang).

[1] Contributed equally to this work, and should be considered as co-first author.

https://doi.org/10.1016/j.isatra.2023.02.010
0019-0578/

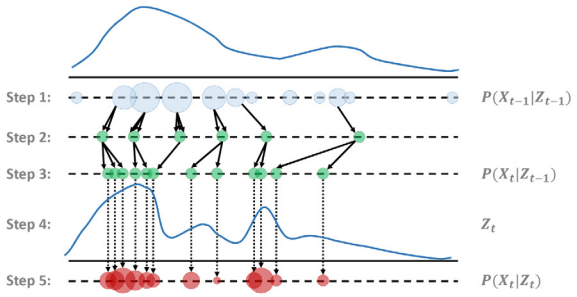

Fig. 1. The process of traditional particle filter. Step 1: Begin with weighted samples from last time; Step 2: Draw samples according to the weights; Step 3: Predict by applying motion model; Step 4: Obtain new measurements; Step 5: Assign weights to particles, proportionally to their likelihood.

has two drawbacks [14]: **particle impoverishment** and **sample-size dependency**. Some academics attempted to come up with solutions by improving resamplings. Tiancheng Li et al. proposed a stratified resampling method [15], and Juha Ala-Luhtala et al. proposed a systematic resampling method [16]. Both two modified resampling methods are built on multi-layered perception. However, the samples decrease after iterations, with only a few occupying most of the weights. As a result, final estimation findings are not always as excellent as intended. Implementing a more competent approach to improve the particle filters' performance is alluring. Quantum computing-inspired optimization (QCiO) has been applied to numerous works for performance enhancement [17].

QCiO is based on the quantum concept, such as superposition and entanglement. As a revolutionary ideology, QCiO has been applied to several applications to obtain optimal results [17]. For example, quantum-inspired particle swarm optimization (QPSO) has presented superiority in obtaining the optimal for many electromagnetic problems [18]. To optimize the expected sum uplink transmit rate without any prior knowledge of ground users, Li et al. [19] proposed a quantum-inspired reinforcement learning (QiRL) approach to solve the trajectory planning problem. In particular, quantum improvement in particle filters also attracted the attention of many researchers. A. Khalili et al. [20] proposed a quantum particle filter for pedestrian tracking. It simulates the uncertainty of the position of electrons around the nucleus by propagating particles in areas where the person is more likely to be. However, the method in [20] lacks quantum theory. It simply modeled the behavior of electrons and improved the prediction process without using quantum theory and mechanisms.

Quantum mechanics deliver comprehensive quadratic speedup for computation [21]. Inspired by quantum mechanics, we proposed a diversity-preserving quantum-inspired particle filter (DQPF). In DQPF, quantum mechanics are applied to improve the property of particles and the resampling process. As we all know, the classical particle can only be in one state at one moment. However, DQPF transforms the classical particles into quantum ones by quantizing the motion patterns, which plays a crucial role in overcoming particle impoverishment and sample-size dependency. Then, Grover's algorithm improves the resampling process. Benefiting from quantum mechanics, the proposed DQPF has better precision and stability with fewer particles than the general one. The contributions of this paper are as follows:

- We apply the quantum superposition to transform classical particles into quantum ones. Quantum representation and corresponding quantum operations are addressed.
- The superposition property of quantum particles avoids the concerns of particle impoverishment and sample-size dependency. The proposed DQPF obtains better accuracy and stability with fewer particles. A smaller sample size also helps to reduce computational complexity.
- The proposed method has significant advantages for abrupt-motion tracking. The quantum particles are propagated at the prediction stage. They will exist at possible places when abrupt motion occurs, which reduces the tracking delay and enhances the tracking accuracy.

The organization of this paper is shown as follows. Firstly, Section 2 puts forward the motion model and the traditional particle filter issues. We also introduce the concept of quantum computation for the understanding of this work. Section 3 first describes the framework of DQPF. Then the representation of quantum particles and Grover's resampling method are presented. In Section 4, the numerical experiments' findings verify the superiority of the proposed DQPF. Section 5 summarizes the paper.

2. Preliminaries

2.1. Motion model

Consider a target node outfitted with an IMU, represented by $\mathcal{M}$. The state transition process and the measurement process are executed in discrete time. The time interval is denoted as t_k, where $k = 0, 1, \ldots, K$. The state space at time t_k is denoted as $\boldsymbol{S}_k$ (see Table 1), which includes vector of coordinate $\boldsymbol{P}_k = [x_k, y_k]^T$ and vector of velocity $\boldsymbol{V}_k = \left[v_x^k, v_y^k\right]^T$. That is to say, $\boldsymbol{S}_k = \left[\boldsymbol{P}_k^T, \boldsymbol{V}_k^T\right]^T$. For the abrupt-motion tracking issue, this paper first offered the dynamic model. The dynamic walking process is assumed to conform to the motion law of node $\mathcal{M}$. Thus, we took advantage of the first-order hidden Markov model and built the dynamic model as follows:

$$\boldsymbol{S}_k = f(\boldsymbol{S}_{k-1}, \boldsymbol{A}_{k-1}, \boldsymbol{\zeta}) \tag{1}$$

where the $\boldsymbol{A}_{k-1}$ represents the vector of acceleration at time t_{k-1} and the $\boldsymbol{\zeta}$ represents the Gaussian noise generated during state transition process. In this paper, $\boldsymbol{A}_k = [a_x^k, a_y^k]^T$ and the value of a_x^k or a_y^k is introduced randomly from $\{0, -g, g\}$, simulated as a random Markov jump [22]. The $\boldsymbol{\zeta} = \left[\zeta_x, \zeta_y\right]^T$ satisfies $\zeta_x, \zeta_y \sim \mathcal{N}(0, \Sigma)$. The target's measurement is given as a state-relate metric in this work. IMU collects information on the target's step distance and heading direction according to the acceleration and angular velocity. The measurement of the step distance at t_k is represented as $\hat{d}_k = d_k + \iota_k$, where $d_k = \sqrt{(x_{k+1} - x_k)^2 + (y_{k+1} - y_k)^2}$ and the noise ι_k satisfies $\iota_k \sim \mathcal{N}(0, \Psi_k)$. The measurement of step distance could be reflected as the vector $\hat{\boldsymbol{d}} = \left[\hat{d}_0, \hat{d}_1, \ldots, \hat{d_{K-1}}\right]^T$. Meanwhile, the measurement of the heading direction at t_k is represented as $\hat{\theta}_k = \theta_k + \vartheta_k$, where $\theta_k = \arctan \frac{y_{k+1} - y_k}{x_{k+1} - x_k}$ and the noise ϑ_k satisfies $\vartheta_k \sim \mathcal{N}(0, \Omega_k)$. The measurement of heading direction could reflected as the vector $\hat{\boldsymbol{\theta}} = \left[\hat{\theta}_0, \hat{\theta}_1, \ldots, \hat{\theta}_{K-1}\right]^T$.

2.2. Quantum computation

Quantum computers are programmable quantum mechanical systems that do computations using quantum physics features. Quantum computing delivers exponential speedups for various computer processes. These speedups are made possible by three quantum physics phenomena: superposition, interference, and entanglement. In quantum computation, qubit is the primary

Table 1
Symbol description.

Symbol	Description	Symbol	Description
$\boldsymbol{S}$	– State space	t_k	– Time interval
$\boldsymbol{P}$	– Vector of coordinate	ι	– Gaussian noise of step distance
$\boldsymbol{V}$	– Vector of velocity	ϑ	– Gaussian noise of heading direction
$\boldsymbol{A}$	– Vector of acceleration	Ψ	– Variance of ι
$\boldsymbol{\zeta}$	– Gaussian noise of process	Ω	– Variance of ϑ
Σ	– Variance of $\boldsymbol{\zeta}$	$\|\psi\rangle$	– Quantum state
d	– Actual step distance	I	– Identity matrix
θ	– Actual heading direction	N_v	– Number of velocity space elements
$\hat{\boldsymbol{d}}$	– Measurement of step distance	O_1	– Quantum oracle
$\hat{\boldsymbol{\theta}}$	– Measurement of heading direction	N_p	– Number of particles

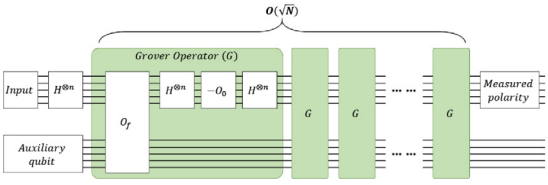

Fig. 2. The framework of Grover's algorithm.

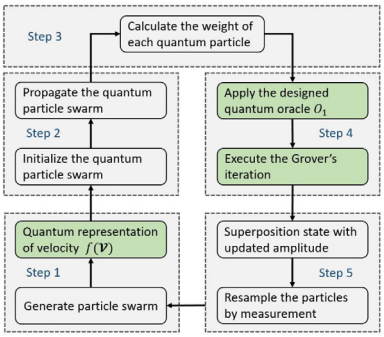

Fig. 3. Framework of DQPF.

object of information carrier, as bit in classical computation. A qubit can be denoted as $|\psi\rangle = \alpha|0\rangle + \beta|1\rangle$, where α and β are called amplitudes and satisfy the normalized equation: $|\alpha|^2 + |\beta|^2 = 1$ [23]. Once a qubit is measured, it will collapse into certain eigenstates. In other words, under the probability of $|\alpha|^2$ or $|\beta|^2$ $|\psi\rangle$ collapses into $|0\rangle$ or $|1\rangle$ after being measured. Further, the quantum mechanics introduces an essential matrix named unitary transformation matrix U. The matrix U is utilized to transform the quantum state $|\psi\rangle$ to different quantum state $|\psi'\rangle$ as $|\psi'\rangle = U|\psi\rangle$. U is required satisfying $U^\dagger U = UU^\dagger \equiv I$, where I represents identity matrix. There are a lot of significant quantum gates designed for a particular operation. More introduction about quantum gates can be found in [23].

Grover's search method is the most well-known quantum method [24], proposed by Lov Grover in 1996. It speeds up the solution to unstructured database searches, requiring fewer steps than any traditional algorithm. Grover represents particular items in quantum forms and applies several unitary operators to manipulate their state iteratively. The framework of Grover's algorithm is shown as Fig. 2. As the primary operations in Grover's search, the Grover iteration will be utilized in the resampling process of the proposed DQPF method.

3. Diversity-preserving quantum-inspired particle filter

In this section, the proposed DQPF is detailed. First, the framework of DQPF is introduced. Next, the representations of quantum particles and the designed quantum operations for improving the quantum particle resampling mechanism are shown. At last, the DQPF's implementation is presented.

3.1. Framework of DQPF

Inspired by quantum mechanics, the property of particles and the resampling process are improved in DQPF. The framework of DQPF is described in Fig. 3. First, the newly classical particle swarm is generated and the particle's velocity is represented using qubits. Then the quantum particle swarm with superposition of velocity is obtained. DQPF propagates quantum particles according to their velocity. Thus the weight of each quantum particle is calculated by measuring the state of the target. Due to the superposition of velocity, the particle's weight is also in a superposition. Next, the designed quantum oracle is applied, and Grover's iteration is executed to mark the high-weight particles. Eventually, the superposition state of a quantum particle with updated amplitude is obtained. The superposition state is measured to collapse, and a new particle swarm is generated for the next tracking iteration.

3.2. Quantum representation of particles

A bit can have a value of 0 or 1, but a qubit can also be a superposition of 0 and 1. Here, in a quantum-inspired particle filter, the classical particles are transformed into quantum particles by utilizing the attribute of the qubit. Although the changes in velocity are continuous, the particle's velocity is quantized. Agreeing to the superposition rule in quantum computation [17], the eigenvelocity at time t_k can be represented in a linear superposition form as follows:

$$|\mathcal{V}_k\rangle = \sum_n \left[\alpha_n|v_x^k\rangle, \beta_n|v_y^k\rangle\right] \tag{2}$$

where α_n and β_n satisfy $\sum_n |\alpha_n|^2 = 1$ and $\sum_n |\beta_n|^2 = 1$, respectively. In this paper, let N_v denote the number of velocity space elements. It is assumed that $N_v = 2^m$ and m indicate the numbers of qubits for velocity. Then Eq. (2) can be rewritten as:

$$|\mathcal{V}_k^{(N_v)}\rangle \to |\mathcal{V}_k^{(m)}\rangle = \sum_{v=\overbrace{00\ldots0}^{m}}^{\overbrace{11\ldots1}^{m}} C_v|v\rangle \tag{3}$$

where C_v is probability amplitudes, and the condition is satisfied:

$$\sum_{v=\overbrace{00\ldots0}^{m}}^{\overbrace{11\ldots1}^{m}} |C_v|^2 = 1.$$

Since classical particles are transformed into quantum particles, one quantum particle could be propagated simultaneously with different velocities to cope with any abrupt change. One quantum particle is equivalent to a swarm of classical particles.

The following subsection will detail the quantum operations of particles, which describes the resampling process with quantum particles.

3.3. Quantum operations of particles

Due to the inapplicability of the traditional unstructured search algorithm for quantum particle space, this paper takes advantage of Grover's search algorithm. The particle resampling process is executed by measuring particles. Since the quantum particle is in a superposition of eigenvelocity, $|v\rangle$ will collapse with the probability $|C_v|^2$ once measurement occurs. Grover's iteration has the ability to amplify the amplitude of a quantum particle's high-weight state. In DQPF, let $f(\boldsymbol{\mathcal{V}}) = |\boldsymbol{\mathcal{V}}_k^{(N_v)}\rangle = |\boldsymbol{\mathcal{V}}_k^{(m)}\rangle$ be the velocity of particle. There are three steps to realize the Grover operator as follows: (1) Initial the superposition of 2^m possible eigenvelocity $|\boldsymbol{\mathcal{V}}_k^{(m)}\rangle$ by the Hadamard matrix as follows:

$$\begin{aligned}|\boldsymbol{\mathcal{V}}_k^{(m)}\rangle &= H^{\otimes m}|\overbrace{00\ldots0}^{m}\rangle = \frac{1}{\sqrt{2^m}}|00\ldots0\rangle + \cdots + |11\ldots1\rangle \\ &= \frac{1}{\sqrt{2^m}}\sum_{x=0}^{2^m-1}|v\rangle\end{aligned} \tag{4}$$

According to the quantum representation of particles, $\frac{1}{\sqrt{2^m}}$ is corresponding to the probability amplitude C_v. The Hadamard transform can be represented as follows:

$$H^{\otimes m} = \frac{1}{\sqrt{2^m}}\begin{bmatrix}1 & 1\\ 1 & -1\end{bmatrix}^{\otimes m} \tag{5}$$

Furthermore, the initial velocity above can be rewritten as:

$$\begin{aligned}f(\boldsymbol{\mathcal{V}}) = |\boldsymbol{\mathcal{V}}_{k,k=0}^{(m)}\rangle &= \frac{1}{\sqrt{2^m}}\sum_{x=0}^{2^m-1}|v\rangle = \frac{1}{\sqrt{2^m}}|v\rangle + \frac{1}{\sqrt{2^m}}\sum_{x\neq v}|x\rangle \\ &= \frac{1}{\sqrt{2^m}}|v\rangle + \frac{\sqrt{2^m-1}}{\sqrt{2^m}}\cdot\frac{1}{\sqrt{2^m-1}}\sum_{x\neq v}|x\rangle = \frac{1}{\sqrt{2^m}}|v\rangle \\ &+ \frac{\sqrt{2^m-1}}{\sqrt{2^m}}|v^{\perp}\rangle\end{aligned} \tag{6}$$

Here, supposed $\frac{1}{\sqrt{2^n}} \equiv \sin\theta$, hence, Eq. (6) can be rewritten as:

$$f(\boldsymbol{\mathcal{V}}) = |v_0^{(m)}\rangle = \sin\theta|v\rangle + \cos\theta|v^{\perp}\rangle \tag{7}$$

(2) Apply the oracle O_1. Denote unitary operator O_1 as a quantum oracle. In the proposed DQPF, the oracle is designed as follows:

$$|\psi_1\rangle : |v_k^{(m)}\rangle \xrightarrow{O_1} \frac{1}{\sqrt{2^m}}\sum_{x=0}^{2^m-1}(-1)^{f(v)}|v\rangle|-\rangle \tag{8}$$

Here $f(v)$ is the condition for whether $|v_k^{(m)}\rangle$ flips or not. If $f(v) = 1$, $|v_k^{(m)}\rangle$ flips. Moreover, the notation $|-\rangle$ represents $|-\rangle = \frac{|0\rangle-|1\rangle}{\sqrt{2^m}}$. (3) Achieve the Grover iteration as follows:

$$|\psi_2\rangle : |\psi_1\rangle \xrightarrow{G} \left[\left(2|v_k^{(m)}\rangle\langle v_k^{(m)}| - I\right)|\psi_1\rangle\right]^{\mathcal{F}} \approx |\boldsymbol{\mathcal{V}}\rangle\frac{|0\rangle-|1\rangle}{\sqrt{2^m}} \tag{9}$$

where G is unitary transformation denoted as:

$$G = O_1\left(2|v_k^{(m)}\rangle\langle v_k^{(m)}| - I\right) \tag{10}$$

And

$$2|v_k^{(m)}\rangle\langle v_k^{(m)}| - I = H^{\otimes m}(2|0\rangle\langle 0| - I)H^{\otimes m} \tag{11}$$

The conditional phase shift is performed by operation $(2|0\rangle\langle 0| - I)$. In addition, $\mathcal{F}$ represents the Grover iteration time. The amplitude of $|v_k^{(m)}\rangle$ will be updated when the quantum particle with velocity $|v\rangle$ is selected. However, we need guarantee $f(v) = 1$ to realize the updating process in Grover's iteration.

At the end of Grover's iteration, the quantum particle is measured, and the superposition of the quantum particle collapses into a definite state by probability amplitude. Then the particle swarm is obtained, which is applied to the next tracking iteration. Since it is transformed into a quantum particle swarm, particle impoverishment will be solved.

3.4. Implementation and complexity

For better illustration, an integrated pseudo-code is shown as in Algorithm 1. Then, we briefly analyze its complexity. Grover's search has an ideal number of iterations N_{optimal} to produce the maximum probability of measuring a valid output. If the problem has p possible terms and q of them are solutions to the problem, then $N_{\text{optimal}} \approx \frac{\pi}{4}\sqrt{\frac{p}{q}}$ (refer to [25]). In DQPF, the most critical parameters that affect the computation time are number of velocity space elements N_v and number of particles N_p. There are N_p solutions from $N_p \times N_v$ items. Then, its complexity is at most $O(\sqrt{\frac{N_p \times N_v}{N_p}}) = O(\sqrt{N_v})$.

4. Numerical simulation and analysis

To test the proposed DQPF, several groups of experiments on the target tracking problem are compared to the other four improved particle filters. Two state-of-the-art classical particle filters: standard Systematic Resampling particle filter (SR) [26] and Compressed Monte Carlo Resampling particle filter (CMCR) [27]. An improved classical particle filter aiming at abrupt-motion tracking problem is also considered, named the Intensively Adaptive Markov-chain Monte Carlo method (IA-MCMC) [28]. In order to explain the advantages of DQPF more comprehensively, we compare it with the existing quantum particle filter [20].

4.1. Experimental setup

This paper conducted the experiments on the platform Azure Quantum, a Microsoft cloud service that includes a different set of quantum solutions. All the experiments are deployed on a personal computer with four core i5 CPU and 16 GB memory, whose operating system is Windows 10 system.

To demonstrate the effectiveness of the DQPF method against the abrupt motion, this paper conducted experiments based on the motion modes of the target, which can be divided as follows:

- **Random motion:** The target might abruptly change its step distance and the heading direction at each step. This means that abrupt motion could occur at each step;
- **Rectangle motion:** The target changes the heading direction 90° counterclockwise every 20 steps, while keeping the step distance unchanged;
- **Traversal motion:** The target keeps the step distance unchanged, moves straight for 10 steps, and then turns back. The abrupt motion occurs when the target turns back;
- **Rectilinear motion:** The target keeps the step distance and the heading direction unchanged. There is no abrupt motion that occurs in rectilinear mode;
- **Circular motion:** The target moves in a uniform circle. There is no abrupt motion that occurs in circular mode.

Algorithm 1 The DQPF algorithm for abrupt-motion tracking.

Input: : The state and the measurement of target, the number of velocity space elements N_v and the number of particles N_p.
Output: : The estimation of target with abrupt-motion.
I. INITIALIZATION AND QUANTIZATION
01. Initialize velocities of N_p classical particles;
02. Map each classical velocity to quantum eigenvelocity $\left|\boldsymbol{\mathcal{V}}^{(N_v)}\right\rangle = \sum_{v=00\ldots0}^{\overbrace{11\ldots1}^{m}} C_v|v\rangle$;
II. PREDICTION
03. Initialize N_p quantum particles according to step 2;
04. Propagate quantum particle according to every $|v\rangle$ with amplitude C_v simultaneously while target moving;
III. WEIGHT CALCULATION
05. Calculate the weight of each $|v\rangle$ according to the measurement of target;
06. Execute the normalization of weights;
IV. GROVER'S RESAMPLING
07. Mark the $|v\rangle$ with high weight as $|\widetilde{v}\rangle$ of each particle;
08. Apply the quantum oracle O_1 to $|\widetilde{v}\rangle$ according to Eq. (8);
09. Achieve the Grover iteration by the unitary transformation G according to Eqs. (9)–(10);
10. Update the amplitude of $|\widetilde{v}\rangle$;
V. QUANTUM MEASURING
11. Measure each quantum particle and the $\left|\boldsymbol{\mathcal{V}}^{(N_v)}\right\rangle$ collapses;
12. Obtain new classical particle swarm for next tracking.

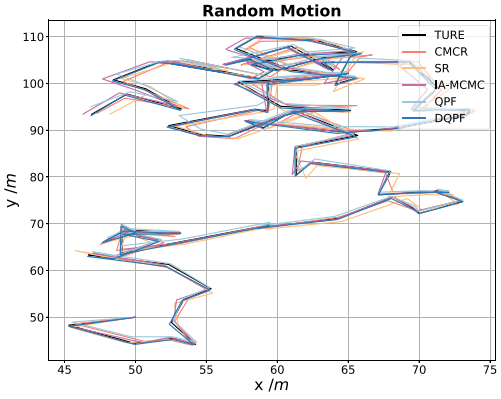

Fig. 4. The random motion trajectory when $N_p = 90$.

The target travels 100 steps at each simulation scenario, and the trajectories are recorded. The other four particle filters (CMCR, SR, IA-MCMC, and QPF) are also performed in each simulation scenario. The accuracy criterion expressed as the Euclidean distance between the estimation and the actual state of the target is defined as follows:

$$error = \left\|\boldsymbol{P}_T - \hat{\boldsymbol{P}}\right\|_2 = \sqrt{\left(x_T - \hat{x}\right)^2 + \left(y_T - \hat{y}\right)^2} \tag{12}$$

where $\|\cdot\|_2$ denotes the Euclidean norm. $\boldsymbol{P}_T{=}[x_T, y_T]^T$ is the actual coordinate and $\hat{\boldsymbol{P}}{=}\left[\hat{x}, \hat{y}\right]^T$ is the estimation. The Euclidean distance clearly describes the estimation deviation from the actual state at each step. After iteration, we performed a statistical calculation on all error samples generated in the iteration process. Statistical results analyze the effectiveness of each algorithm in each scenario.

As we all know, the traditional particle filter algorithm's accuracy depends on sample size [14]. However, the computation efficiency decreases tremendously when setting a large sample size. The proposed DQPF solves this problem. In our simulation, we changed the number of particles N_p to execute experiments to verify the effectiveness of DQPF. The number of particles gradually increases, and then the error trends of the five filtering algorithms are observed.

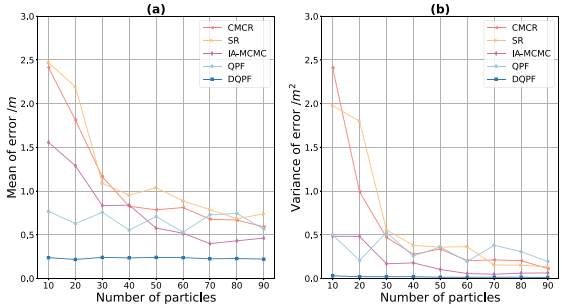

Fig. 5. The random motion error.

4.2. Random motion simulation

Fig. 4 visually shows the random motion trajectory (take the situation when $N_p = 90$, for example). As can be seen, the target is moving erratically. The abrupt motion almost occurs at each step. Fig. 5 shows the error trends of the five filtering algorithms as the number of particles increases. Fig. 5-(a) and -(b) visually show the trends of mean and variance of error samples, respectively.

As N_p increases, the average error and the corresponding standard deviation of CMCR, SR, and IA-MCMC show a gradually decreasing trend, as shown in Fig. 5. It proves that the accuracy and stability of traditional particle filters depend on the sample size. The larger sample size makes the estimation more accurate and stable. As a traditional particle filter aiming at abrupt motion tracking problems, IA-MCMC outperforms the other two in performance. The maximum average error of IA-MCMC 1.56 m is less than corresponding values of CMCR and SR when $N_p = 10$. The superiority of IA-MCMC is not affected by the change in particle number.

As shown in Fig. 5, QPF's average error and corresponding standard deviation always fluctuate. This proves that the QPF is almost unaffected by particle number. The QPF's accuracy is better than classical particle filters when N_p is small. However, classical methods, especially IA-MCMC, gradually outperform QPF in performance as N_p increases. For example, the average error and the corresponding standard deviation of IA-MCMC are less than the corresponding values of QPF when $N_p > 50$. This proves that the advantages of QPF are limited and can be surpassed by classical algorithms.

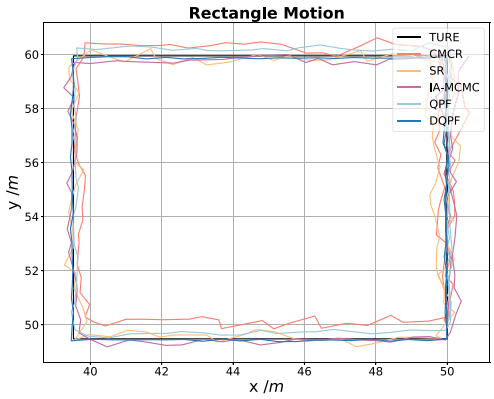

Fig. 6. The rectangle motion trajectory when $N_p = 90$.

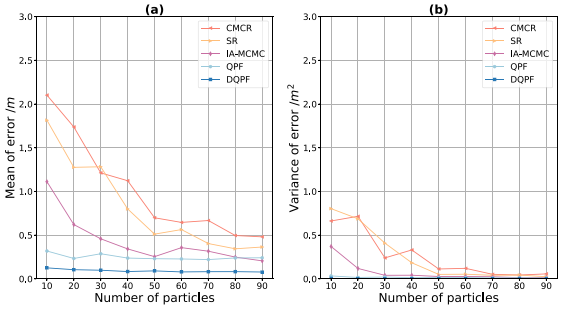

Fig. 7. The rectangle motion error.

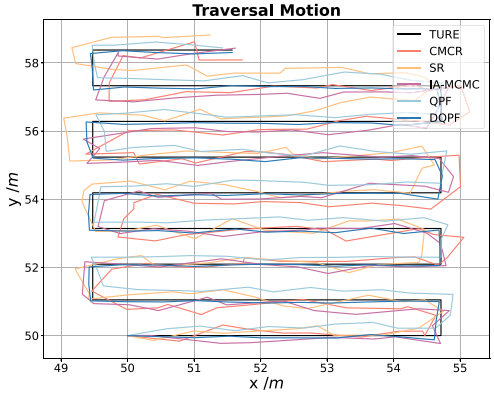

Fig. 8. The traversal motion trajectory when $N_p = 90$.

As for the proposed DQPF, the average error and the corresponding standard deviation keep relatively stable in Fig. 5. This indicates that DQPF is not only not affected by particle number but also has good stability. Moreover, its performance obviously outperforms the other four methods in accuracy and stability. Above all, the proposed DQPF is insensitive to the number of particles. Furthermore, it reaches a more accurate estimation with fewer particle numbers, which indicates the superiority of DQPF for random motion.

4.3. Rectangle motion simulation

Fig. 6 visually shows the rectangle motion trajectory (take the situation when $N_p = 90$, for example). As can be seen, the target changes the heading direction 90° counterclockwise every 20 step. The abrupt motion only occurs when the target changes the heading direction counterclockwise. Fig. 7 shows the error trends of the five filtering algorithms as the number of particles increases. Fig. 7-(a) and -(b) visually show the trends of mean and variance of error samples, respectively.

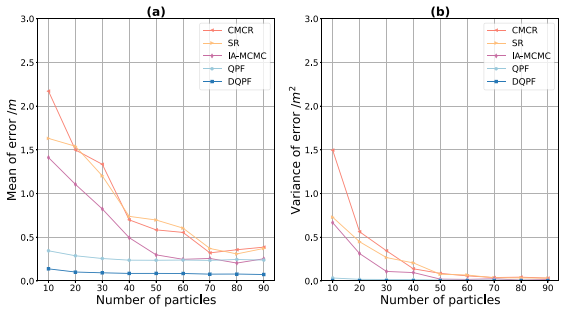

Fig. 9. The traversal motion error.

In terms of three classical particle filters, the average error and the corresponding standard deviation show a gradually decreasing trend as N_p increases, as shown in Fig. 6. This phenomenon is similar to random motion, which depends on the sample size. However, all three classical algorithms in the rectangular mode are improved compared with the random mode. For example, the maximum average error of SR 1.82 m is less than the corresponding values in the random mode. It can be seen that although the frequency of abrupt motion is reduced, the effect on the general classical filtering algorithm is still adverse. Nevertheless, the classical algorithm can adapt to regular motion.

Regarding QPF, the accuracy and stability have improved than the random mode's. As shown in Fig. 6, there is no significant fluctuation, which differs from Fig. 5. Furthermore, the maximum average error of QPF 0.32 m is smaller than the minimum average error 0.53 m in the random mode. Besides, QPF is almost always superior to classical particle filters. It proves that QPF can deal with motion mode with a low frequency of abrupt motion.

As for the proposed DQPF, the average error and the corresponding standard deviation keep relatively stable. Like QPF, the accuracy and stability have improved than the random mode's. The average error of DQPF remains at around 0.10 m, while the standard deviation holds steady. Compared with QPF, DQPF has more advantages in precision and stability. This once again proves the effectiveness of DQPF.

4.4. Traversal motion simulation

Fig. 8 visually shows the traversal motion trajectory (take the situation when $N_p = 90$, for example). As can be seen, the target keeps the step distance unchanged, moves straight for 10 steps, and then turns back. The abrupt motion occurs when the target turns back. Fig. 9 shows the error trends of the five filtering algorithms as the number of particles increases. Fig. 9-(a) and -(b) visually show the trends of mean and variance of error samples, respectively.

In traversal mode, the frequency of abrupt motion is mainly up-regulated than in rectangle mode, as shown in Fig. 8. In terms of five improved particle filters, the error trends in this mode are similar to the one in rectangle mode, which can be analyzed simply by comparing Fig. 9 with Fig. 7. The traversal and rectangle motion share a common characteristic: an occasional abrupt movement occurs after a period of regular movement. This also often happens in daily life. It can be analyzed that the proposed DQPF is more accurate and stable than other particle filters in motion mode with occasional abrupt motion in daily life.

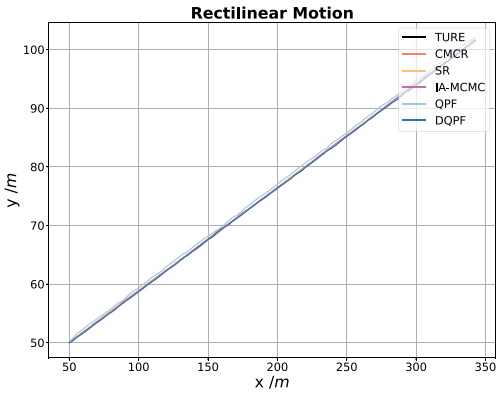

Fig. 10. The rectilinear motion trajectory when $N_p = 90$.

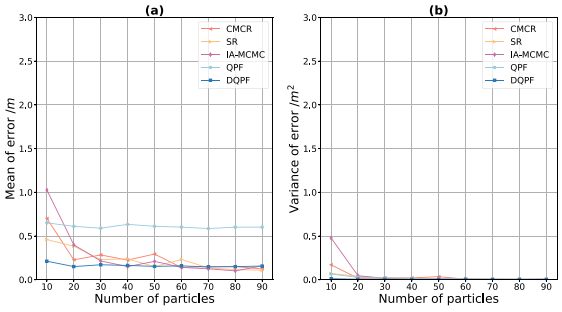

Fig. 11. The rectilinear motion error.

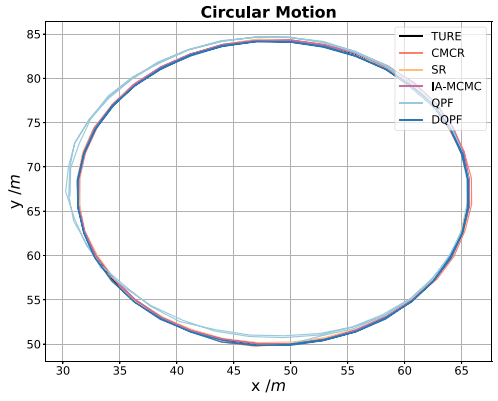

Fig. 12. The circular motion trajectory when $N_p = 90$.

4.5. Rectilinear motion simulation

Fig. 10 visually shows the rectilinear motion trajectory (take the situation when $N_p = 90$, for example). As can be seen, the target keeps the step distance and the heading direction unchanged. There is no abrupt motion that occurs in rectilinear mode. Fig. 11 shows the error trends of the five filtering algorithms as the number of particles increases. Fig. 11-(a) and -(b) visually show the trends of mean and variance of error samples, respectively.

Although QPF maintains good stability in rectilinear mode, it does not seem to be as accurate as in rectangle or traversal mode. For example, the average error of QPF remains at around 0.61 m, while the corresponding value holds steady at around 0.26 m. It proves that QPF is not good at motion mode with no abrupt motion.

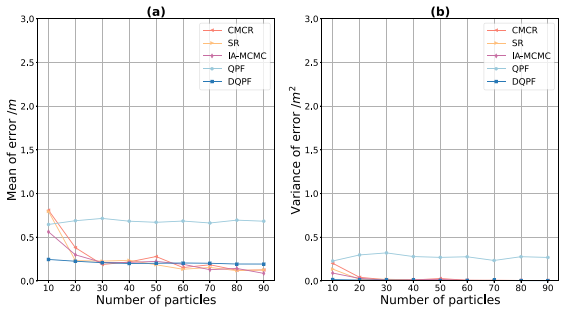

Fig. 13. The circular motion error.

All three classical particle filters have a good performance. Their accuracy and stability gradually approach DQPF as N_p increases, as shown in Fig. 11. This demonstrates that the classical particle filter is sufficient to solve the tracking problem of regular motion when N_p is sufficient. However, the proposed DQPF still shows excellent performance and is independent of sample size in rectilinear motion. The average error of DQPF remains at around 0.17 m, while the standard deviation holds steady. This proves that DQPF is also suitable for regular motion.

4.6. Circular motion simulation

Fig. 12 visually shows the circular motion trajectory (take the situation when $N_p = 90$, for example). As can be seen, the target moves in a uniform circle. There is no abrupt motion that occurs in circular mode. Fig. 13 shows the error trends of the five filtering algorithms as the number of particles increases. Fig. 13-(a) and -(b) visually show the trends of mean and variance of error samples, respectively.

As we all know, uniform circular motion is also a regular motion. It can be seen that the error trends in this mode are similar to the ones in rectilinear mode, which can be analyzed simply by comparing Fig. 13 with Fig. 11. Regarding QPF, the variance of the error sample has increased overall than the corresponding value in rectilinear mode. This illustrates the limitations of QPF.

Moreover, all three classical particle filters a little outperform the proposed DQPF when $N_p > 50$. On the one hand, it can be explained that the classical methods are more adaptive to regular motion when particle number is enough. On the other hand, there is some probability that the quantum particle collapses in a low-probability state. It harms the performance of regular motion tracking. Even so, DQPF still has excellent accuracy and stability, especially in solving the problem of abrupt motion tracking.

4.7. Computational complexity analysis

The computational complexity of classical particle filters is $O(N_p)$ according to the big O notation [26–28]. It declares that the particle number severely influences the classical particle filters' complexity. As we all know, the classical particle filter has a trade-off between precision and complexity. If the particle number is insufficient, it is challenging for particles to estimate the actual state after multiple iterations. Nevertheless, the system's real-time requirements cannot be guaranteed by enlarging the particle number. However, as mentioned in Section 3, the computational complexity of DQPF is at most $O(\sqrt{N_v})$. It declares that the particle number does not influence the computation efficiency of the proposed DQPF. The complexity is only up to the number of velocity space elements. Since DQPF satisfies the condition $\sqrt{N_v} \ll N_p$, its computational complexity is superior to classical particle filter. The more accurate estimation can be

obtained once the values of N_v and N_p are appropriate in DQPF, and meanwhile, the real-time requirements of the system are met.

5. Conclusions

This paper proposed a new modified particle filter method DQPF which avoids the problems of particle impoverishment and sample-size dependency by introducing quantum characteristics. We apply the concept of quantum superposition to transform classical particles into quantum particles. Quantum representation and corresponding quantum operations are come up to utilize quantum particles. The superposition property of quantum particles avoids the concerns of particle impoverishment and sample-size dependency. The proposed DQPF obtains better accuracy and stability with fewer particles. A smaller sample size also helps to reduce computational complexity. Moreover, it has significant advantages for abrupt-motion tracking. The quantum particles are propagated at the prediction stage. They will exist at possible places when abrupt motion occurs, which reduces the tracking delay and enhances the tracking accuracy. Numerical experimental results demonstrated that the DQPF is not susceptible to motion mode and particle number while maintaining excellent accuracy and stability. Our future work will focus on in-depth theoretical research on the convergence of DQPF and other quantum-inspired algorithms.

Declaration of competing interest

The authors declare that they have no known competing financial interests or personal relationships that could have appeared to influence the work reported in this paper.

Acknowledgment

This work is supported in part by National Natural Science Foundation of China (NSFC) under Grant 62101029.

References

[1] Yuan Y, Lu Y, Wang Q. Tracking as a whole: Multi-target tracking by modeling group behavior with sequential detection. IEEE Trans Intell Transp Syst 2017;18(12):3339–49. http://dx.doi.org/10.1109/tits.2017.2686871.
[2] Xu C, Chai D, He J, Zhang X, Duan S. Innohar: A deep neural network for complex human activity recognition. IEEE Access 2019;1.
[3] Jang B, Kim H. Indoor positioning technologies without offline fingerprinting map: A survey. IEEE Commun Surv Tutor 2019;21(1):508–25. http://dx.doi.org/10.1109/COMST.2018.2867935.
[4] Zafari F, Gkelias A, Leung KK. A survey of indoor localization systems and technologies. IEEE Commun Surv Tutor 2019;21(3):2568–99.
[5] Shi J, Wang G, Jin L. Moving source localization using TOA and FOA measurements with imperfect synchronization. Signal Process 2021;186:108113.
[6] Xiong W, Schindelhauer C, So HC, Bordoy J, Gabbrielli A, Liang J. TDOA-based localization with NLOS mitigation via robust model transformation and neurodynamic optimization. Signal Process 2021;178:107774.
[7] Shi J, Wang G, Jin L. Least squared relative error estimator for RSS based localization with unknown transmit power. IEEE Signal Process Lett 2020;27:1165–9. http://dx.doi.org/10.1109/LSP.2020.3005298.
[8] Zhang H, Zhang X, Wang Y, Shi K, Zhang J, Li C. An experimental comparison of swarm optimization based abrupt motion tracking methods. IEEE Access 2018;6:75383–94.
[9] Zhang H, Gao Z, Ma X, Zhang J, Zhang J. Hybridizing teaching-learning-based optimization with adaptive grasshopper optimization algorithm for abrupt motion tracking. IEEE Access 2019;7:168575–92.
[10] Lebeda K, Hadfield S, Matas J, Bowden R. Texture-independent long-term tracking using virtual corners. IEEE Trans Image Process 2015;25(1):359–71.
[11] Kwon J, Lee KM. Wang-Landau Monte Carlo-based tracking methods for abrupt motions. IEEE Trans Pattern Anal Mach Intell 2012;35(4):1011–24.
[12] Duan S, Wu H, Xu C, Wan J. Toward swarm robots tracking: a constrained gaussian condensation filter method. In: Advances in swarm intelligence, 12th international conference, ICSI 2021, Qingdao, China, July 17–21, 2021, proceedings, Part II. 2021.
[13] Xu C, Wang X, Duan S, Wan J. Spatial-temporal constrained particle filter for cooperative target tracking. J Netw Comput Appl 2021;176:102913. http://dx.doi.org/10.1016/j.jnca.2020.102913.
[14] Fu X, Jia Y. An improvement on resampling algorithm of particle filters. IEEE Trans Signal Process 2010;58(10):5414–20.
[15] Li T, Bolic M, Djuric PM. Resampling methods for particle filtering: Classification, implementation, and strategies. IEEE Signal Process Mag 2015;32(3):70–86. http://dx.doi.org/10.1109/MSP.2014.2330626.
[16] Ala-Luhtala J, Whiteley N, Heine K, Piché R. An introduction to twisted particle filters and parameter estimation in non-linear state-space models. IEEE Trans Signal Process 2016;64(18):4875–90. http://dx.doi.org/10.1109/TSP.2016.2563387.
[17] Biamonte J, Wittek P, Pancotti N, Rebentrost P, Wiebe N, Lloyd S. Quantum machine learning. Nature 2017;549(7671):195–202. http://dx.doi.org/10.1038/nature23474.
[18] Tu S, Rehman OU, Rehman SU, Ullah S, Waqas M, Zhu R. A novel quantum inspired particle swarm optimization algorithm for electromagnetic applications. IEEE Access 2020;8:21909–16. http://dx.doi.org/10.1109/ACCESS.2020.2968980.
[19] Li Y, Aghvami AH, Dong D. Intelligent trajectory planning in UAV-mounted wireless networks: A quantum-inspired reinforcement learning perspective. IEEE Wireless Commun Lett 2021;10(9):1994–8. http://dx.doi.org/10.1109/LWC.2021.3089876.
[20] Khalili A, Soliman A-H, Asaduzzaman M. Quantum particle filter: a multiple mode method for low delay abrupt pedestrian motion tracking A. Khalili , A.A. Soliman and M. Asaduzzaman. Electron Lett 2015;51:1251–3. http://dx.doi.org/10.1049/el.2015.1013.
[21] Hu W, Hu J. Training a quantum neural network to solve the contextual multi-armed bandit problem. Nat Sci 2019.
[22] Li W, Yang Z, Hu H. Sequential particle-based sum-product algorithm for distributed inference in wireless sensor networks. IEEE Trans Veh Technol 2012;62(1):341–8.
[23] Dong D, Petersen IR. Quantum control theory and applications: a survey. IET Control Theory Appl 2010;4(12):2651–71.
[24] Godfrin C, Ferhat A, Ballou R, Klyatskaya S, Ruben M, Wernsdorfer W, Balestro F. Operating quantum states in single magnetic molecules: implementation of Grover's quantum algorithm. Phys Rev Lett 2017;119(18):187702.
[25] Vinod GM, Shaji A. Finding solutions to the integer case constraint satisfiability problem using Grover's algorithm. IEEE Trans Quant Eng 2021;2:1–13. http://dx.doi.org/10.1109/TQE.2021.3120449.
[26] Tian Q, Wang KI-K, Salcic Z. An INS and UWB fusion approach with adaptive ranging error mitigation for pedestrian tracking. IEEE Sens J 2020;20(8):4372–81. http://dx.doi.org/10.1109/JSEN.2020.2964287.
[27] Martino L, Elvira V. Compressed Monte Carlo with application in particle filtering. Inform Sci 2021;553:331–52. http://dx.doi.org/10.1016/j.ins.2020.10.022.
[28] Zhou X, Lu Y, Lu J, Zhou J. Abrupt motion tracking via intensively adaptive Markov-chain Monte Carlo sampling. IEEE Trans Image Process 2012;21(2):789–801. http://dx.doi.org/10.1109/TIP.2011.2168414.